J|A|C|S
ARTICLES
Published on Web 01/23/2007

Quantifying the Sequence-Dependent Species Barrier between Hamster and Mouse Prions

Lily Y.-L. Lee and Rita P.-Y. Chen*

Contribution from the Institute of Biological Chemistry, Academia Sinica, No. 128, Sec 2, Academia Road, Nankang, Taipei 115, Taiwan, Republic of China

Received September 19, 2006; E-mail: pyc@gate.sinica.edu.tw

Abstract: Prion diseases are transmissible neurodegenerative disorders. It is widely accepted that prions are the infectious agents responsible for disease transmission, and the sequence homology between the infectious prion and the host prion protein determines its transmission efficiency across species. However, previous studies have often reported different results regarding seeding efficiency, the efficiency of initiating amyloid propagation by adding pre-existing amyloid fibrils as seed. In the present study, we used synthetic peptides as a simple system to determine the sequence-dependent transmission barrier between hamster and mouse. We found that the heterologous seeding efficiency of hamster and mouse prion peptides was 4 times less than that of homologous seeding. Moreover, residue 139 was not the only residue in determining seeding efficiency. When the seed had Ile at this position, the homology at this position between seed and monomer determined the seeding efficiency. When the seed had Met at this position, homology at residues 109 and 112 determined the seeding efficiency.

Introduction

Prion diseases, fatal transmissible neurodegenerative diseases of mammals,[1−3] are also known as transmissible spongiform encephalopathies (TSEs). "Prion" stands for "proteinaceous infectious particle" discovered in the disease-transmitting material from infectious brain tissues and named by Prusiner.[4] The prion is a misfolded isoform of a constantly expressed protein named prion protein (PrP). The structural conversion of PrP from the cellular native isoform (PrP^C) to the disease-causing isoform (PrP^{Sc}) results in disease. PrP^{Sc} is partially protease-resistant and so accumulates in the cell, leading to cell death.

In the 1930s, a massive epidemic of sheep scrapie due to vaccination against louping ill suggested scrapie could be transmitted. In the 1940s, Cuillé and Chelle[5] demonstrated that scrapie is an infectious disease by the successful transfer of scrapie from sheep to goats. The transmission properties of prions were not widely studied until Chandler successfully transmitted scrapie to mice and established animal models for measuring the transmission titer.[6] Although transmission has been proved possible, transmission efficiencies between different animals are quite varied. It has been established that the transmission barrier for prion diseases, often called the "species barrier", is related to differences in the primary sequences of PrP between the inoculum and the host (especially within sequence 90−145 of the PrP).[7−12] However, in work exploring the species barrier, differences are often obtained. How to evaluate the sequence-dependent transmission barrier is an interesting challenge in prion studies.

Hamster and mouse prions are the most common systems used for studying the species barrier. However, contradictory results have been obtained using different experimental designs. In 1995, Priola and Chesebro[13] used mouse prion to infect mouse neuroblastoma cells which expressed recombinant mouse or hamster PrP and showed that the mouse PrP, but not the hamster PrP, could be seeded by mouse prion and that a single hamster-specific amino acid, Met-139, inhibited the conversion. On the other hand, Kocisko et al.[14] used a cell-free system to explore the molecular basis of the species barrier. They converted mouse or hamster PrP^C into the protease-resistant form by incubating it with mouse or hamster PrP^{Sc} in the presence of denaturants and showed that mouse PrP^C could be seeded only by mouse PrP^{Sc}, whereas hamster PrP^C could be seeded by both. Recently, Vanik et al. used recombinant PrP23−144 (prion protein sequence 23−144)[15] to test sequence-dependent fibrillization and seeding specificity[16] and found that the hamster PrP23−144 monomer could only be seeded by hamster PrP23−144

(1) Chesebro, B. *Br. Med. Bull.* **2003**, *66*, 1−20.
(2) Prusiner, S. B. *Proc. Natl. Acad. Sci. U.S.A.* **1998**, *95*, 13363−13383.
(3) Aguzzi, A.; Polymenidou, M. *Cell* **2004**, *116*, 313−327.
(4) Prusiner, S. B. *Science* **1982**, *216*, 136−144.
(5) Cuille, J.; Chelle, P.-L. *C. R. Acad. Sci.* **1939**, *208*, 1058−1060.
(6) Chandler, R. L. *Lancet* **1961**, *277*, 1378−1379.
(7) Supattapone, S.; Bosque, P.; Muramoto, T.; Wille, H.; Aagaard, C.; Peretz, D.; Nguyen, H. O.; Heinrich, C.; Torchia, M.; Safar, J.; Cohen, F. E.; DeArmond, S. J.; Prusiner, S. B.; Scott, M. *Cell* **1999**, *96*, 869−878.
(8) Kaneko, K.; Peretz, D.; Pan, K.; Blochberger, T.; Wille, H.; Gabizon, R.; Griffith, O.; Cohen, F.; Baldwin, M.; Prusiner, S. *Proc. Natl. Acad. Sci. U.S.A.* **1995**, *92*, 11160−11164.
(9) Supattapone, S.; Bouzamondo, E.; Ball, H. L.; Wille, H.; Nguyen, H. O.; Cohen, F. E.; DeArmond, S. J.; Prusiner, S. B.; Scott, M. *Mol. Cell. Biol.* **2001**, *21*, 2608−2616.
(10) Baskakov, I. V.; Aagaard, C.; Mehlhorn, I.; Wille, H.; Groth, D.; Baldwin, M. A.; Prusiner, S. B.; Cohen, F. E. *Biochemistry* **2000**, *39*, 2792−2804.
(11) Harrison, P. M.; Bamborough, P.; Daggett, V.; Prusiner, S. B.; Cohen, F. E. *Curr. Opin. Struct. Biol.* **1997**, *7*, 53−59.
(12) Huang, Z.; Prusiner, S. B.; Cohen, F. E. *Folding Des.* **1996**, *1*, 13−19.
(13) Priola, S. A.; Chesebro, B. *J. Virol.* **1995**, *69*, 7754−7758.
(14) Kocisko, D. A.; Priola, S. A.; Raymond, G. J.; Chesebro, B.; Lansbury, P. T., Jr.; Caughey, B. *Proc. Natl. Acad. Sci. U.S.A.* **1995**, *92*, 3923−3927.
(15) Kundu, B.; Maiti, N. R.; Jones, E. M.; Surewicz, K. A.; Vanik, D. L.; Surewicz, W. K. *Proc. Natl. Acad. Sci. U.S.A.* **2003**, *100*, 12069−12074.

10.1021/ja0667413 CCC: $37.00

Table 1. Prion Peptides Used[a]

name of the peptide[b]	sequence			
	109 112			139
MMM	NMKHMAGAAA	AGAVVGGLGG	YMLGSAMSRP	MMHFGND
LVI	NLKHVAGAAA	AGAVVGGLGG	YMLGSAMSRP	MIHFGND
MMI	NMKHMAGAAA	AGAVVGGLGG	YMLGSAMSRP	MIHFGND
LVM	NLKHVAGAAA	AGAVVGGLGG	YMLGSAMSRP	MMHFGND

[a] The variant residues are underlined. The residue number is according to the sequence number of the hamster prion protein. [b] MMM, peptide containing hamster prion protein amino acids 108−144; LVI, peptide containing mouse prion protein amino acids 107−143; MMI, MMM with a Met → Ile substitution at residue 139; LVM, LVI with an Ile → Met substitution at residue 138.

amyloid fibrils, whereas the corresponding mouse PrP23−144 monomer could be seeded by amyloid fibrils from both sources. Moreover, although mouse PrP23−144 amyloid fibrils could not serve as seed to initiate the fibrillization of the hamster PrP23−144 monomer, mouse PrP23−144 amyloid fibrils that had been seeded by hamster PrP23−144 amyloid fibrils were able to do so.

The hamster and mouse PrPs have 94% sequence identity, and there are only three different residues within the amyloidogenic sequence 90−145. The hamster PrP has Met at positions 109, 112, and 139, while the mouse PrP has Leu, Val, and Ile at the corresponding positions (Table 1). It has been reported that Met-139 is the key residue determining the seeding efficiency of the hamster and mouse prions.[13] Priola et al.[17] also found that the homology at residue 155 also influences the seeding efficiency of the hamster prion, but homology at the same position has little effect on the seeding efficiency of the mouse prion. Jones and Surewicz[18] proposed that amyloids from different species adopt different secondary structures and morphologies and that the amino acid residue at position 139 was closely related to the structural differences. Whether residue 139 affects the seeding efficiency through the resulting fibril structure and whether other residues also contribute remain to be determined.

Amyloid has a cross β-sheet structure. This particular structural feature gives rise to special spectroscopic signals in UV, fluorescence, and circular dichroism (CD) spectroscopy. According to the nucleation-dependent polymerization model (Figure 1), amyloid formation has a lag phase in which nucleation takes place. The spectroscopic signal is very small during this stage, but a large signal change is seen during the fast polymerization catalyzed by the nuclei. The nuclei serve as seed in the propagation phase, and the signal change derived from the structural conversion is proportional to the concentrations of the seed and monomer:

$$dS/dt = Ak_e[\text{seed}]_t[\text{monomer}]_t + Bk_n[\text{monomer}]_t^x \quad (1)$$

where S is the signal arising from cross-β structure formation when monomers are incorporated into the amyloid structure, A and B are constants, k_e is the polymerization rate constant, k_n is the nucleation rate constant, x is the monomer concentration dependency during nucleation, and $[\text{seed}]_t$ and $[\text{monomer}]_t$ are the molar concentrations of seed and monomer in its "ready-to-stack" state, or called "β-precursor state", at time t, respectively. For spontaneous amyloidogenesis, the concentration of seed gradually increases during the lag time until a critical concentration is reached which allows elongation to occur (bottom panel, top section). If seed is added exogenously during the lag time (bottom panel), the lag time is shortened to different extents (bottom panel, bottom section) or even completely eliminated (bottom panel, center section), depending on the amount of added seed.[19,20] Thus, in studies exploring seeding specificity, the amount of seed used is very important. In seeding experiments, when the supplied seed concentration is much higher than the critical seed concentration required for both homologous and heterologous monomers, the lag time-free propagation seen in both cases will lead to an incorrect conclusion of no specificity. On the other hand, when the seed concentration is lower than the critical seed concentration required for the heterologous monomer but higher than that for the homologous monomer, the large lag time difference will suggest a large species barrier between the homologous and heterologous monomers. Different amounts of seed should therefore be used to compare the real seeding efficiencies.

Here, we used a seed titration method to evaluate the seeding barrier between hamster and mouse prions. Peptides corresponding to hamster PrP residues 108−144 and mouse PrP residues 107−143 were used as a model system. In order to examine the correlation between seeding efficiency and protein sequence, in addition to the hamster and mouse prion peptides, peptides corresponding to the hamster prion peptide with a Met-139 → Ile substitution or to the mouse prion peptide with an Ile-139 (number adopted from the hamster PrP sequence) → Met substitution were also studied.

Experimental Methods

Peptide Synthesis. The prion peptides were prepared by the batch Fmoc−polyamide method.[21] The N-terminal end of the peptide was acetylated and the C-terminal end amidated in order to mimic polypeptide bonds in the full-length protein. After deprotection and purification, the peptides were characterized by mass spectroscopy, lyophilized, and stored at −20 °C.

Circular Dichroism (CD) Spectroscopy. The peptide was dissolved at the indicated concentration in 20 mM NaOAc, 140 mM NaCl, pH 3.7, and the solution was incubated at the indicated temperature. After different incubation times, samples were put in a 1-mm cell, and the CD spectra between 200 and 250 nm were recorded on a J-715 CD spectrometer (JASCO, Japan). The bandwidth was set to 2 nm, and the step resolution was 0.05 nm. Three scans were averaged for each sample.

Thioflavin T (ThT) Binding Assay. A stock solution of 5 mM thioflavin T (ThT) was prepared by dissolving the dye (2 mg) in 1.25 mL of 140 mM NaCl, 100 mM phosphate buffer, pH 8.5 and filtering the solution through a 0.22 μm Millipore filter. A fresh working solution was prepared by adjusting the final dye concentration to 200 μM. A 30 μL aliquot of sample was mixed with 30 μL of 200 μM ThT dye solution for 1 min at room temperature, then the fluorescence emission between 460 and 600 nm was measured in a 3-mm path length rectangular cuvette on an FP-750 spectrofluorometer (JASCO, Japan) with excitation at 442 nm.

(16) Vanik, D. L.; Surewicz, K. A.; Surewicz, W. K. *Mol. Cell* **2004**, *14*, 139−145.
(17) Priola, S. A.; Chabry, J.; Chan, K. *J. Virol.* **2001**, *75*, 4673−4680.
(18) Jones, E. M.; Surewicz, W. K. *Cell* **2005**, *121*, 63−72.
(19) Krebs, M. R. H.; Morozova-Roche, L. A.; Daniel, K.; Robinson, C. V.; Dobson, C. M. *Protein Sci.* **2004**, *13*, 1933−1938.
(20) Bocharova, O. V.; Breydo, L.; Salnikov, V. V.; Gill, A. C.; Baskakov, I. V. *Protein Sci.* **2005**, *14*, 1222−1232.
(21) Chen, P. Y.; Lin, C. K.; Lee, C. T.; Jan, H.; Chan, S. I. *Protein Sci.* **2001**, *10*, 1794−1800.

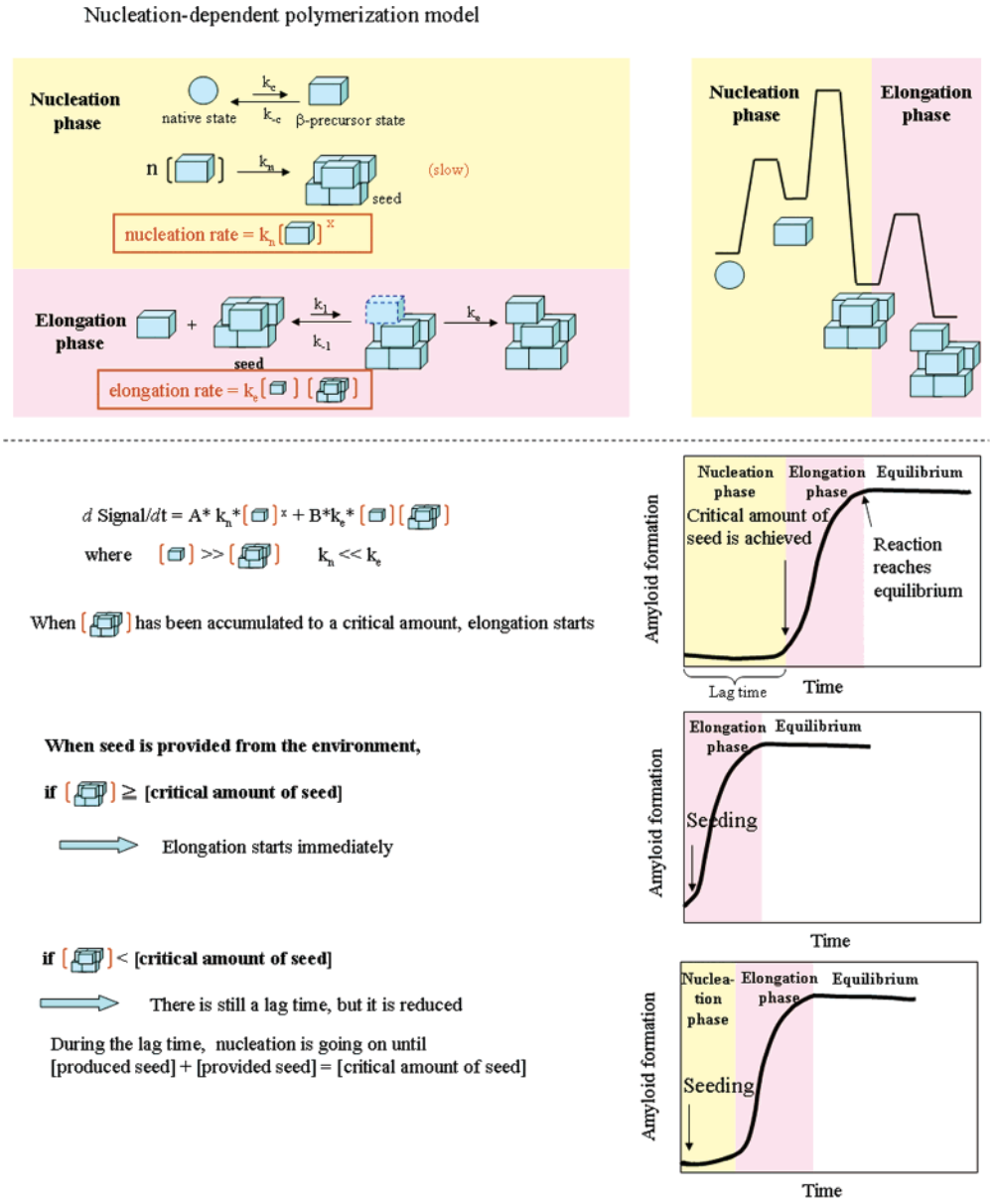

Figure 1. Nucleation-dependent polymerization model for amyloidogenesis. The native state of the protein (peptide in our case) is represented by ○. For a protein to form amyloid, it must be able to undergo structural conversion to a "ready-to-stack" state (β-precursor state, represented by □). The energy diagram of these states is presented on the top right. In the nucleation-dependent polymerization model, the formation of nuclei (seed) is the rate-determining step (top panel, top section). Nucleation dominates the process for spontaneous amyloidogenesis (yellow background). The time required for nuclei formation is called the lag time. However, the signal change due to nuclei formation is very small, as its concentration is much smaller than that of the monomer. When the amount of nuclei reaches a critical concentration, elongation, the second phase (pink background) starts to take over, resulting in an abrupt change in the amyloid formation curve (bottom panel, top section). The nuclei can be added exogenously (seeding) (bottom panel, center and bottom sections). If the added seed amount is equal to, or higher than, the critical seed concentration (bottom panel, center section), the propagation phase starts immediately. If the acquired seed amount is lower than the critical seed concentration (bottom panel, bottom section), the nucleation step continues until the critical concentration is reached.

Preparation of Seed. The peptide was dissolved at a concentration of 75 μM in 20 mM NaOAc, and 140 mM NaCl, pH 3.7, and the solution was incubated at 25 °C for amyloidogenesis until equilibrium was achieved, as indicated by no change in CD signal. The amyloid fibrils were then spun down in an Eppendorf tube and resuspended in distilled water. The fibril suspension was fragmented with 20 cycles of intermittent pulses (five pulses of 0.5 s each; 5 s interval between each cycle) using an ultrasonic processor (UP100H, Hielscher, U.S.A.) equipped with a 1-mm microtip immersed in the sample. The power setting was fixed at 40%.

Seed Titration Method. For seeding experiments, the peptide solution (62.5 μM) was prepared in 25 mM NaOAc and 175 mM NaCl, pH 3.7. Volumes of up to 50 μL of the sonicated seed solution were added to 200 μL of each peptide solution and the total volume made to 250 μL with distilled water, giving a final monomer concentration of 50 μM. The kinetics of fibril formation at room temperature within 100 min was monitored by time-resolved CD spectroscopy immediately after the seed was mixed with the monomers. The CD signal at 218 nm was recorded every 5 s. The same batch of seed was used throughout the experiments. Different quartz cuvettes were used for different samples to avoid cross contamination.

Electron Microscopy. The peptides were dissolved in 20 mM NaOAc, 140 mM NaCl, pH 3.7 and incubated to form amyloid fibrils. Sample negative staining was performed on Formvar- and carbon-coated 300-mesh copper grids. Samples were loaded onto the grid and left for 4 min for absorption, then stained with 2% uranyl acetate for another

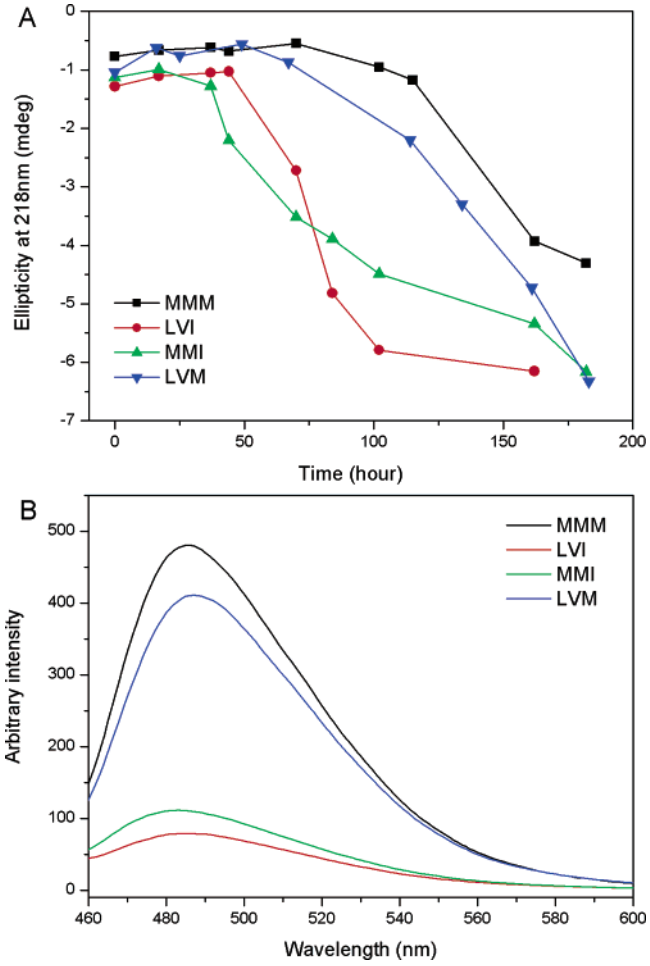

Figure 2. (A) Time course of amyloidogenesis of four prion peptides monitored by CD spectroscopy. The peptides were dissolved at a final concentration of 25 μM in 20 mM NaOAc, 140 mM NaCl, pH 3.7 and incubated at 30 °C for the indicated time. (B) ThT fluorescence spectra for the fibrils formed by the prion peptides after the amyloidogenesis reaction reached equilibrium. The peptides were dissolved at a final concentration of 50 μM in 20 mM NaOAc, 140 mM NaCl, pH 3.7 and incubated at 25 °C for 2 weeks before performing the ThT binding assay.

4 min. After overnight drying in a desiccator, the samples were viewed in a JEOL-2010 electron microscopy (JEOL, Japan) at 200 kV.

Results

Amyloidogenesis of the Prion Peptides. Despite their sequence homology (Table 1), the mouse and hamster prion peptides differed markedly in their ability to form amyloid fibrils and in terms of the morphology of the fibrils. The hamster prion peptide (denoted the MMM peptide, a peptide containing hamster prion protein amino acids 108−144) had a longer lag time (Figure 2A) and usually formed long fibrils with two protofibrils twisted together (Figure 3A). In contrast, the mouse prion peptide (denoted the LVI peptide, a peptide containing mouse prion protein amino acids 107−143) had a short lag time and the fibrils usually formed tangles, or plaques (Figure 3B). To examine the correlation between the amino acid sequence and the kinetics of amyloidogenesis, residue 139 of the hamster and mouse prion peptides was switched (denoted the MMI (MMM with a Met → Ile substitution at residue 139) and LVM (LVI with an Ile → Met substitution at residue 138) peptides, respectively) and amyloid formation examined. The results showed that the lag time of the MMI peptide was as short as

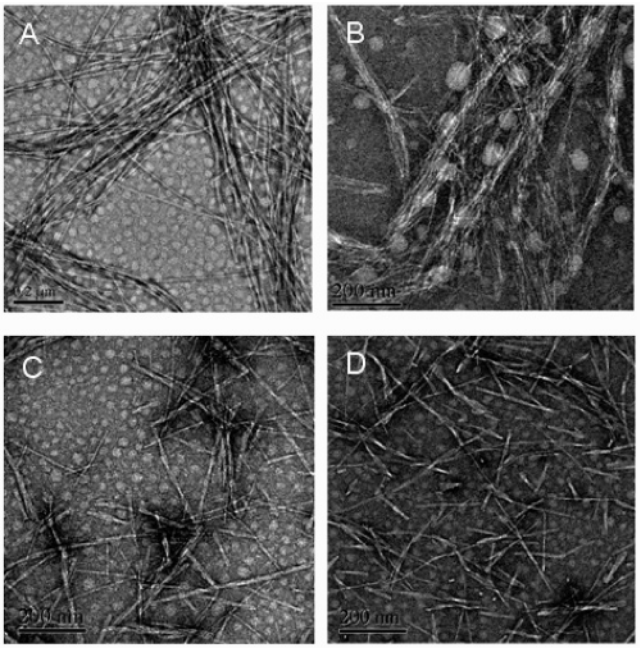

Figure 3. EM images of the amyloid fibrils: (A) MMM fibrils, (B) LVI fibrils, (C) sonicated MMM fibrils, and (D) sonicated LVI fibrils. The scale bars correspond to 200 nm.

that of the LVI peptide and that of the LVM peptide was as long as that of the MMM peptide. These results show that residue 139 is the most important factor determining the nucleation rate. Peptides with Ile at this position more readily formed nuclei than peptides with Met at the same site. This is not altogether surprising, since residue 139 is close to the kink region we reported previously.[22] Any mutation or modification close to this kink region could change the accessibility of the polypeptide chain in the β-precursor state, and the β-precursor state population greatly influences nucleus formation. In the case of the mouse prion peptide, the presence at position 139 of Ile, which is branched at the β-carbon and has a higher propensity than Met to form β-sheet structure, clearly speeded up the nucleation step by stabilizing the β-conformers, which are the activated precursors in the formation of the nucleus.

Interestingly, at the same concentration, the prion peptides showed different fluorescence intensities in the ThT binding assay (Figure 2B), with amyloid fibrils formed from the MMM and LVM peptides showing extraordinarily high fluorescence emission. It is not clear whether the side chains of the Met residue at position 139 directly affect the ThT fluorescence or whether the conformation of the formed amyloid fibrils leads to the difference. Due to this great fluorescence difference, amyloid formation in our seeding experiments was monitored by CD spectroscopy instead of ThT fluorescence emission.

Seeding Experiments. Traditional strategies for measuring and comparing prion transmission efficiency include (1) comparing the number of affected animals and the incubation period for animals showing symptoms of prion disease after prion inoculation,[7,23,24] (2) comparing the SDS−PAGE band intensity of the protease-resistant part of PrP^{Sc} (usually named PrP^{res})

(22) Chen, P. Y.; Lin, C. C.; Chang, Y. T.; Lin, S. C.; Chan, S. I. *Proc. Natl. Acad. Sci. U.S.A.* **2002**, *99*, 12633−12638.
(23) Hill, A. F.; Desbruslais, M.; Joiner, S.; Sidle, K. C. L.; Gowland, I.; Collinge, J.; Doey, L. J.; Lantos, P. *Nature* **1997**, *389*, 448−450.

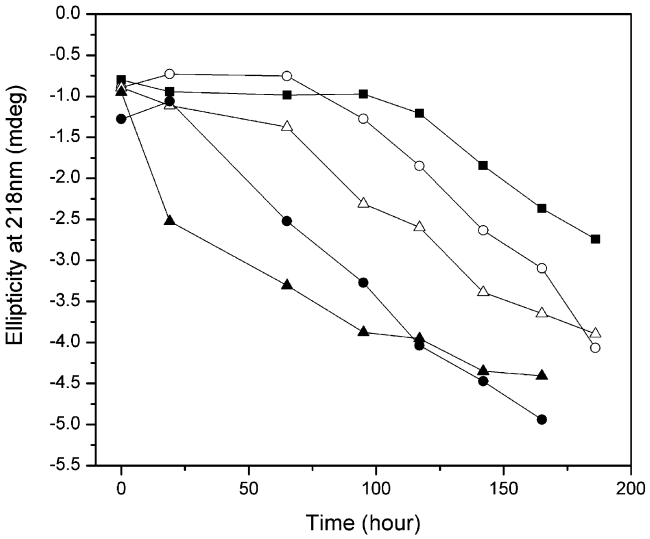

Figure 4. Seeding experiments. To prepare the seed solution, the MMM and LVI peptides were dissolved at a final concentration of 75 μM in 20 mM NaOAc, 140 mM NaCl, pH 3.7 and incubated at 25 °C until equilibrium was reached. The amyloid fibrils were spun down by centrifugation and resuspended in water; half were used as seed without further treatment, and the other half were sonicated to make a more homogeneous seed solution. MMM peptide at a concentration of 25 μM in the same buffer was used as the unseeded control (■) and incubated at 30 °C, and the kinetics of amyloidogenesis was monitored by CD spectroscopy. For homologous seeding, 100 μL of the sonicated (▲) or unsonicated (●) MMM seed solution was added to 1 mL of MMM peptide solution. For heterologous seeding, 100 μL of the sonicated (△) or unsonicated (○) LVI seed solution was added to 1 mL of MMM peptide solution. The total amounts of amyloid fibrils in the sonicated MMM and LVI seed solutions were determined by their CD ellipticities at 218 nm and were adjusted to the same value by adding water. The same volumes were used for the corresponding unsonicated MMM and LVI fibril suspensions.

from scrapie-infected mouse neuroblastoma cells expressing the desired prion protein,[13,17] (3) mixing a certain amount of prion with purified or expressed PrP^C and comparing the SDS−PAGE band intensity of the produced PrP^{res},[14,25] and (4) mixing a fixed amount of in vitro prepared amyloid fibrils with recombinant PrP and comparing the kinetics of amyloidogenesis using the ThT binding assay.[16,26] In such studies, the amount of the prion seed is not qualitatively and quantitatively controlled. In our seeding studies, we found that the molar concentration of the seed greatly influenced seeding efficiency. Figure 4 shows the amyloidogenesis kinetics of the hamster peptide MMM seeded with seed solution prepared by different methods. The amyloid fibrils were first separated from the precursors by centrifugation. When the fibrils were simply resuspended in water by pipetting up and down, addition of this resulting seed solution to the MMM peptide reduced the lag time. In comparison, when the same amount of fibril solution was fragmented by ultrasonication, the resulting seed solution was more efficient in accelerating amyloidogenesis and the lag time was greatly shortened or even completely eliminated. This greater efficiency of the sonicated material was observed for both homologous and heterologous seeding. These results show that it is the amount of available free ends, rather than of total protein, in the seed solution which determines the seeding efficiency.

Seed Titration Method. The breaking up of aggregates is important for efficient autocatalytic prion amplification, and ultrasonication has been used to amplify prions by breaking pre-existing prions to increase the molar concentration of the seed.[27−30] To use a constant molar concentration of the seed, ultrasonication was used to prepare homogeneous seed. Figure 3, parts C and D, shows EM images of the sonicated fibrils and demonstrates that the clumps of fibrils were dispersed after sonication, but the structural morphology of the fibrils was maintained. It should be noted that the same batch of seed should be used throughout a seeding experiment.

Figure 5 shows a homologous seeding experiment using the hamster peptide MMM. Sonicated MMM fibrils were prepared, and different amounts were used as seed to induce amyloid formation of different concentrations of the same peptide monomer. With the use of 25 μM MMM peptide, a lag time was observed unless at least 15 μL of seed solution was used. As the peptide concentration was increased, less seed was required to immediately initiate amyloid propagation. The minimum required amount of seed for lag time-free propagation was 15, 7.5, and 5 μL at monomer concentrations of 25, 50, and 75 μM, respectively, confirming the reciprocal relationship between the concentrations of monomer and seed.

For heterologous seeding, the elongation rate constant is smaller due to weaker association at the heterologous interface. Accordingly, more seed should be supplied or the lag phase extended until more seed are formed endogenously. However, the lag phase is difficult to measure accurately, prolonged observations can lead to sedimentation of the fibrils, and fragmentation can occur when samples are repetitively taken out and put back for measurements, and thus the molar concentration of the seed can change. In the seed titration experiment, we aimed to determine the critical seed concentration for the same seed and different monomers in the absence of spontaneous nucleation (incubation time of only 1 h) by comparing the kinetics of samples with an identical monomer concentration and different amounts of seed by adding different volumes of seed solution and adjusting the volume with distilled water. The critical seed concentration (minimum required seed amount for lag time = 0) was determined by noting when a continuous decrease in CD $\text{ellipticity}_{(218nm)}$ was seen within the first hour, i.e., when the lag phase disappeared. Cross-species seeding efficiency was quantified as the ratio of the amount of seed required to avoid a lag time in the homologous seeding experiment to that in the heterologous seeding experiment ($[\text{seed}]_{homo}/[\text{seed}]_{hetero}$).

Measuring Cross-Species Seeding Efficiency. Different volumes of sonicated MMM fibrils (made to 50 μL with distilled water) were added to MMM, LVI, MMI, and LVM peptide solutions (final peptide concentration 50 μM). Figure 6A shows that the lag time for the MMM peptide solution was about 5000 s when seeded with 5 μL of MMM fibril solution and that instant amyloid propagation occurred when the seed volume was

(24) Scott, M. R.; Will, R.; Ironside, J.; Nguyen, H.-O. B.; Tremblay, P.; DeArmond, S. J.; Prusiner, S. B. *Proc. Natl. Acad. Sci. U.S.A.* **1999**, *96*, 15137−15142.
(25) Horiuchi, M.; Priola, S. A.; Chabry, J.; Caughey, B. *Proc. Natl. Acad. Sci. U.S.A.* **2000**, *97*, 5836−5841.
(26) Baskakov, I. V. *J. Biol. Chem.* **2004**, *279*, 7671−7677.
(27) Saborio, G. P.; Permanne, B.; Soto, C. *Nature* **2001**, *411*, 810−813.
(28) Piening, N.; Weber, P.; Giese, A.; Kretzschmar, H. *Biochem. Biophys. Res. Commun.* **2005**, *326*, 339−343.
(29) Soto, C.; Saborio, G. P.; Anderes, L. *Trends Neurosci.* **2002**, *25*, 390−394.
(30) Sarafoff, N. I.; Bieschke, J.; Giese, A.; Weber, P.; Bertsch, U.; Kretzschmar, H. A. *J. Biochem. Biophys. Methods* **2005**, *63*, 213−221.

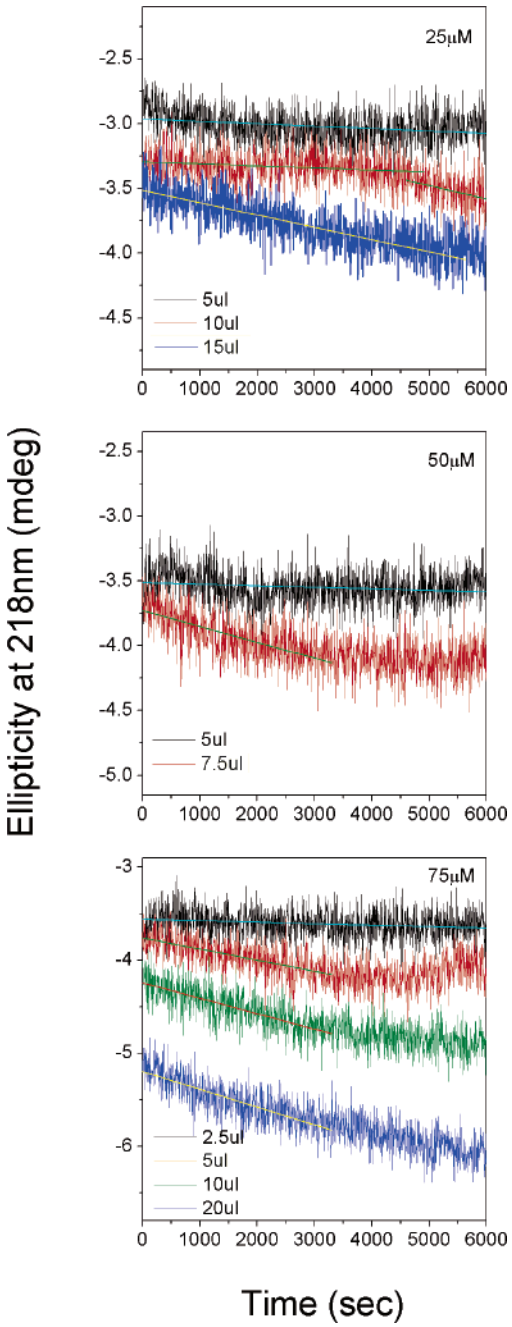

Figure 5. Amyloidogenesis using different concentrations of MMM peptide solution. MMM peptide solutions at final concentrations of 25, 50, or 75 μM were seeded by adding different volumes (indicated on the figure) of the sonicated MMM fibrils (made to 50 μL with distilled water), and amyloid formation was monitored by time-resolved CD spectroscopy at 218 nm. The initial propagation traces were fitted linearly to help identify the lag time. The minimum required seed volume for lag phase-free propagation is highlighted in yellow.

increased to 10 μL (top left panel). In contrast, 40 μL was the minimum MMM seed volume for the LVI peptide (bottom left panel), and the cross-species seeding efficiency of MMM → LVI was therefore one-quarter (10/40) of that for the homologous seeding. This is not surprising, as the residues at position 139 are different. However, MMM → MMI seeding was as efficient as homologous seeding, since only 10 μL of seed was needed to eliminate the lag time (top right panel), while the MMM → LVM seeding efficiency was very low (bottom right panel), despite their sequence homology at residue 139. The

Table 2. Seeding Efficiencies of the Peptides MMM, LVI, MMI, and LVM to the Seed Formed from These Four Peptides

	seed			
monomer	MMM	LVI	MMI	LVM
MMM	1	0.25	0.25	0.25
LVI	0.25	1	1	1
MMI	1	1	1	0.25
LVM	0.2	0.25	0.17	1

seeding efficiency of the MMM fibrils using the various peptides was MMM = MMI > LVI > LVM (minimum required seed volume for lag time-free propagation 10, 10, 40, and 50 μL, respectively). The prion susceptibility ($[seed]_{homo}/[seed]_{hetero}$) of these peptides to MMM fibrils can be quantified as 10/10:10/10:10/40:10/50 = 1:1:0.25:0.2 for the MMM:MMI:LVI:LVM peptide solutions. Our data suggest that, when MMM fibrils were used as seed, sequence homology at residues 109 and 112 determined the seeding efficiency.

When LVI fibrils were used as seed, different results were obtained. As shown in Figure 6B, 2.5 μL of LVI seed caused lag time-free amyloid formation using LVI peptide solution, while 10 μL was required using LVM peptide solution. Similarly, 2.5 μL of LVI seed efficiently initiated amyloid formation using MMI peptide, but 10 μL was required for MMM peptide. On the basis of the minimum amount of seed required to eliminate the lag phase (2.5, 2.5, 10, or 10 μL for peptide LVI, MMI, LVM, or MMM), the prion susceptibility of peptides LVI, MMI, LVM, or MMM to LVI amyloid fibrils was 1, 1, 0.25, or 0.25, respectively. The MMM peptide solution required 4 times more seed solution than the LVI peptide solution, consistent with the MMM fibril seeding studies. However, in contrast to the MMM fibril seeding experiment, residue 139 played a key role in cross-species seeding efficiency when LVI fibrils were used as seed.

When MMI fibrils were used as seed, the minimum required seed volume for immediate amyloid propagation was 2.5, 2.5, 10, or 15 μL for MMI, LVI, MMM, or LVM peptide solutions, respectively (Figure 6C), and the prion susceptibility of these peptides to MMI amyloid fibrils was 1, 1, 0.25, and 0.17, respectively. On the basis of our data, we conclude that, when position 139 of the seed is occupied by Ile, peptides with Ile at the same position have the highest prion susceptibility. For peptides with Met at this site, the transmission barrier is higher and is even higher when residues 109 and 112 of the monomer peptide are also different from those in the seed.

Residue 139 was not the only factor determining seeding efficiency. When residue 139 of the seed was Met, the dominating factor was the homology at positions 109 and 112. In Figure 6D, when LVM fibrils were used as seed, the minimum required seed volume for immediate amyloid propagation for the LVM, LVI, MMM, or MMI peptide solution was 5, 5, 20, or 20 μL, resulting in a seeding efficiency of 1, 1, 0.25, or 0.25. Homology at residues 109 and 112 greatly affected seeding efficiency. Interestingly, this phenomenon is consistent with the results in the MMM seeding experiment, i.e., residue 139 of the monomer peptide did not seem to influence the seeding efficiency at all when residue 139 in the seed was Met. The results of the seeding experiments are summarized in Table 2.

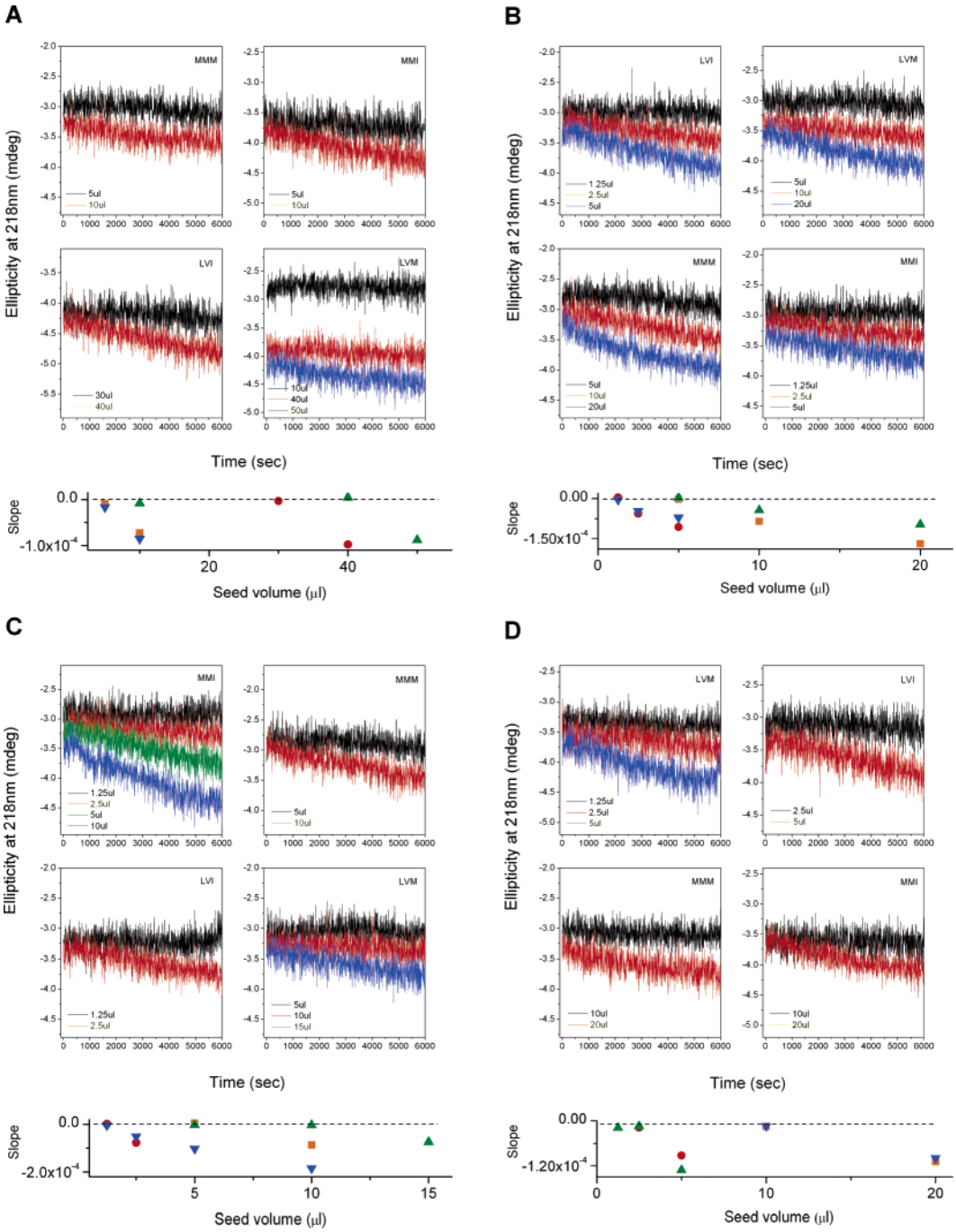

Figure 6. Amyloidogenesis of different prion peptides seeded with sonicated fibrils. The indicated volumes of the sonicated seed (made to 50 μL with distilled water) were added to MMM, LVI, MMI, or LVM peptide solutions (final concentration 50 μM), and the kinetics of amyloidogenesis was monitored by time-resolved CD spectroscopy at 218 nm. The minimum required seed volume for lag phase-free propagation is highlighted in yellow. It should be noted that the same volume of different seed solutions may contain different amounts of seed, so results with different seed cannot be compared: (A) MMM seed, (B) LVI seed, (C) MMI seed, and (D) LVM seed. The initial slopes of the traces are summarized in the bottom plot of each panel: orange, MMM peptide; red, LVI peptide; blue, MMI peptide; green, LVM peptide.

Discussion

According to the nucleation-dependent polymerization model, the rate-determining step in amyloidogenesis consists of a lag phase during which nuclei (seed) are formed. The propensity to form seed is proportional to the population of molecules in the β-conformation. In the case of the prion protein, which has a stable three-dimensional structure, the population in the "ready-to-stack" β-conformation (β-precursor state) will be very small or the structural conversion rate will be very low; therefore, the lag time is very long. For example, the sporadic prion disease, Creutzfeldt Jacob disease, has a late onset (>50 years) and occurs at a low frequency of one in a million. In vitro, the nucleation step can be accelerated by adding denaturant to the buffer to destabilize the PrP^C structure.[26,31] In the propagation phase, monomers must first bind to a nucleus to undergo irreversible structural rearrangement as described by the "dock and lock" mechanism.[25,32] Thus, the available binding surface and the association rate constant determine amyloid

(31) Kocisko, D. A.; Come, J. H.; Priola, S. A.; Chesebro, B.; Raymond, G. J.; Lansbury, P. T.; Caughey, B. *Nature* **1994**, *370*, 471−474.

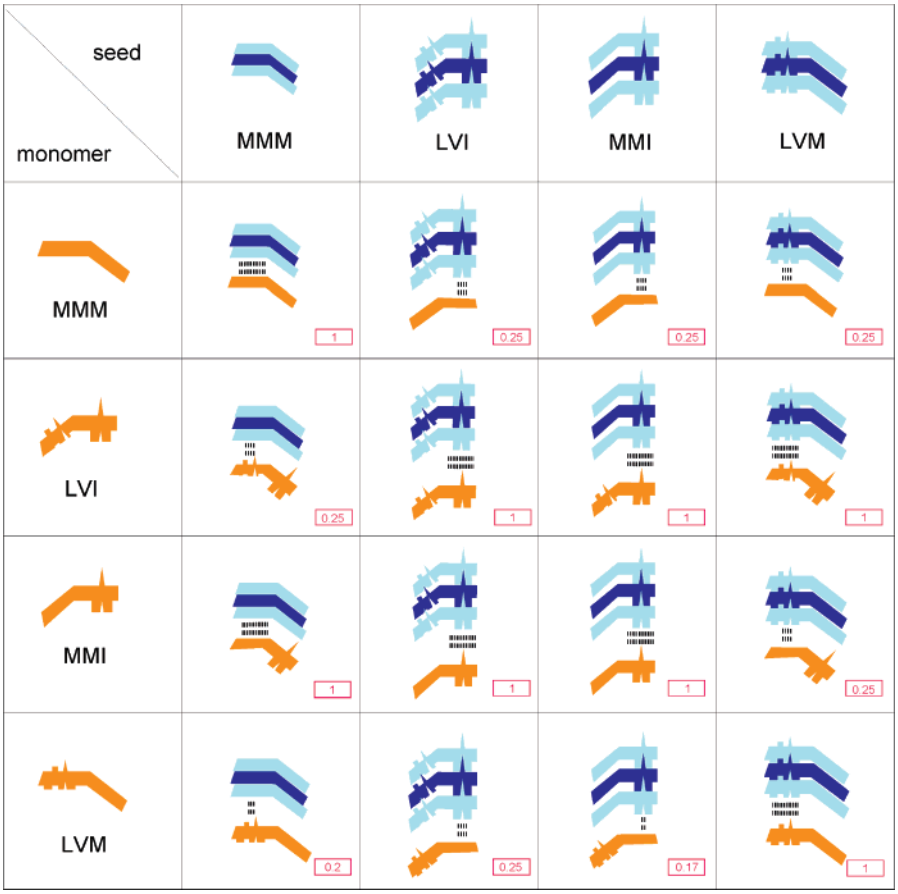

Figure 7. "Convertible binding surface" hypothesis to explain the sequence-dependent seeding efficiency. The density of the dotted lines between the seed and monomer proportionally represents the strength of the binding affinity between them. The experimentally determined seeding efficiency (normalized to homologous seeding) for each seeding experiment is shown in a box. When residue 139 of the seed is Ile, the binding surface is in the C-terminal of the prion peptide. The seeding efficiency is good if the monomer also has Ile at this position. When residue 139 of the seed is Met, the binding surface is in the N-terminal of the prion peptide and the sequence homology between the N-terminal part of the seed and monomer determines the cross-species seeding efficiency.

propagation. When the seeding efficiency is determined by the amount of amyloid formation over a fixed incubation time, it can lead to wrong conclusions because (1) the intrinsic properties of various prion monomers in endogenous seed formation and polymerization rate could be different and (2) the active surface of different seed or different batches of seed from the same species (i.e., the molar concentration of seed) may not be constant throughout the experiment.

Here, we developed a seed titration method to explore the correlation between the amino acid sequence and seeding efficiency in amyloidogenesis. This method is fast and reproducible. The experiments done by recording a CD spectrum at different time points instead of using time-resolved CD spectroscopy acquired the same conclusions (see the Supporting Information). A 37 residue prion peptide was used in this system because of its amyloidogenetic property. To maintain the same molar concentration of the seed, the amyloid fibrils were fragmented by ultrasonication and the same batch of fragmented fibrils used throughout the seeding experiments. The critical amount of seed for each monomer is inversely proportional to its association rate constant. In the seeding process, the association rate constant for the homologous monomer is believed to be higher than that for the heterologous monomers, explaining why the critical amount of seed was lower for homologous seeding. The ratio of the critical amount of seed for the homologous monomer and that for the heterologous monomer may correlate with the barrier to prion transmission. Using this method, we compared the transmission barrier between hamster and mouse and concluded that homology at residue 139 was a critical, but not an absolute, factor in determining seeding efficiency. Interestingly, it seems that residue 139 determines the binding surface between the seed and the incoming monomer. When residue 139 of the seed is Ile, the N-terminal of the peptide (at least residues 109−112) is probably not involved in the association step. In contrast, when it is Met, the homology of the N-terminal sequence 109−112 determines the binding affinity in the association step.

We therefore propose a "convertible binding surface" hypothesis to explain how the amino acid sequence affects prion transmission (Figure 7). During the seeding experiment, the binding surface of the seed is different for different prion peptides. In amyloid fibrils formed from peptides with Ile at position 139, the bulky size of Ile-139, which has β-branching, probably dominates peptide assembly into amyloid and the binding surface is therefore mainly in the C-terminal part of the peptide, and homology in this region determines cross-species seeding efficiency. However, in amyloid fibrils formed from peptides with Met at position 139, the binding surface for

(32) Esler, W. P.; Stimson, E. R.; Jennings, J. M.; Vinters, H. V.; Ghilardi, J. R.; Lee, J. P.; Mantyh, P. W.; Maggio, J. E. *Biochemistry* **2000**, *39*, 6288−6295.

peptide assembly is changed to the N-terminal part of the peptide and sequence homology between seed and monomer in the N-terminal region (residue 109 and 112) determines cross-species seeding efficiency. Due to these differences in the binding surface in the presence of Met or Ile, the structures of the propagated amyloid fibrils of these peptides are probably different. Recently, Jones and Surewicz[18] demonstrated sequence-dependent differences in the secondary structure of amyloid fibrils formed from PrP23−144 by Fourier transform infrared spectroscopy. Proteins with Met at position 139, including hamster PrP23−144 or human PrP23−144 with the Ile-139 → Met mutation, had a very strong β-sheet band at 1625 cm^{-1}, whereas proteins with Ile at position 139, including human PrP23−144, mouse PrP23−144, and hamster PrP23−144 with the Met-139 → Ile mutation, had another band pattern. Moreover, atomic force microscopy showed that fibrils formed from proteins with Ile at position 139 have a "beadlike" morphology, whereas those formed from proteins with Met at this position appear as "smooth" fibrils (∼90%) or have a left-handed helical twist (∼10%). Their results are consistent with our data.

"Strain" phenomenon in prion transmission has been extensively discussed. Different strains are often associated with the intrinsic properties of the prion, such as transmission efficiency, structural stability, susceptibility to protease digestion, and the distribution of various glycosylated forms. Temperature and mutation can alter the strains of the yeast [PSI+] prion.[33,34] Diaz-avalos et al.[35] used "mass per length" measurement by scanning transmission electron microscopy to characterize four morphologies of yeast amyloid fibrils and found that, when seeded by different strains of yeast prion, the distribution of these four morphologies varied. Recently, the three-dimensional structure of Alzheimer Aβ(1−42) fibrils was obtained using quenched hydrogen/deuterium exchange NMR.[36] However, the tertiary interactions in this structure are different from those in a previous proposed model of Aβ(1−40) fibrils.[37] This suggests that a two-residue extension at the C-terminal end of the peptide can alter the hydrophobic binding surface during amyloid propagation. Since prion formation is the assembly of the protein in its "β-precursor state" rather than the native state, any mutations, modifications, or environmental changes, such as temperature, pH, ionic strength, etc., that could alter the β-precursor state conformation will lead to different amyloid structure, as shown in the fibrillation studies of glucagons.[38] Thus, the binding surface or the amyloid core of the prion could be different, even for the same polypeptide chain.

Conclusions

In conclusion, our seed titration approach is an excellent method for quantifying the prion transmission barrier in vitro. Our data showed that residue 139 is not the only critical factor determining cross-species seeding efficiency for prion peptide 108−144. When residue 139 is Met, sequence homology at residues 109 and 112 becomes important. Taken together, our findings argue that the binding surface between the seed and monomer in the seeding reaction depends on the amino acid sequence of the seed. Different protein or peptide sequences might have different binding surfaces. Depending on the conformation of the β-precursor state in each condition, the same protein or peptide could have different binding surfaces, resulting in different strains.

Acknowledgment. We are thankful for the financial support from Academia Sinica and the National Science Council, Taiwan (NSC 94-2311-B-001-007).

Supporting Information Available: Results of seeding experiments repeated by recording one CD spectrum every 20 min, shown in Figures S1−S4 (Figure S1, MMM seed; Figure S2, LVI seed; Figure S3, MMI seed; Figure S4, LVM seed); seeding efficiencies, summarized in Table S1. This material is available free of charge via the Internet at http://pubs.acs.org.

JA0667413

(33) Tanaka, M.; Chien, P.; Naber, N.; Cooke, R.; Weissman, J. S. *Nature* **2004**, *428*, 323−328.
(34) Chien, P.; DePace, A. H.; Collins, S. R.; Weissman, J. S. *Nature* **2003**, *424*, 948−951.
(35) Diaz-Avalos, R.; King, C. Y.; Wall, J.; Simon, M.; Caspar, D. L. *Proc. Natl. Acad. Sci. U.S.A.* **2005**, *102*, 10165−10170.
(36) Luhrs, T.; Ritter, C.; Adrian, M.; Riek-Loher, D.; Bohrmann, B.; Dobeli, H.; Schubert, D.; Riek, R. *Proc. Natl. Acad. Sci. U.S.A.* **2005**, *102*, 17342−17347.
(37) Petkova, A. T.; Ishii, Y.; Balbach, J. J.; Antzutkin, O. N.; Leapman, R. D.; Delaglio, F.; Tycko, R. *Proc. Natl. Acad. Sci. U.S.A.* **2002**, *99*, 16742−16747.
(38) Pedersen, J. S.; Dikov, D.; Flink, J. L.; Hjuler, H. A.; Christiansen, G.; Otzen, D. E. *J. Mol. Biol.* **2006**, *355*, 501−523.